Synthesis and Self-Assembly of β-Octa[(4-Diethoxyphosphoryl)phenyl]porphyrins

Anton Shukaev, Elizaveta Ermakova, Yuanyuan Fang, Karl Kadish, Sergey Nefedov, Victor Tafeenko, Julien Michalak, Alla G. Bessmertnykh-Lemeune

Synthesis and self-assembly of β-octa[(4-diethoxyphosphoryl)phenyl]porphyrins

Anton V. Shukaev,[1] Elizaveta V. Ermakova,*,[2] Yuanyuan Fang,[3] Karl M. Kadish,*,[3] Sergey E. Nefedov,[4] Viktor A. Tafeenko,[5] Julien Michalak[1] and Alla Bessmertnykh-Lemeune*,[1,6]

[1] *Institut de Chimie Moléculaire de l'Université de Bourgogne, Université Bourgogne Franche-Comté, CNRS UMR 6302, 9 Avenue Alain Savary, BP 47870, Dijon 21078 CEDEX, France*

[2] *Frumkin Institute of Physical Chemistry and Electrochemistry, Russian Academy of Sciences, Leninsky Pr. 31-4, Moscow 119071, Russia*

[3] *Department of Chemistry, University of Houston, Houston, Texas 77204-5003, United States*

[4] *N.S. Kurnakov Institute of General and Inorganic Chemistry of Russian Academy of Sciences, Leninsky pr. 31, Moscow 119071, Russia*

[5] *Department of Chemistry, M.V. Lomonosov Moscow State University, 1-3 Leninskie Gory, Moscow 11999, Russia*

[6] *Laboratoire de Chimie, UMR 5182, CNRS, ENS de Lyon, 46 allée d'Italie, CEDEX, 69364 Lyon, France*

ABSTRACT

The β–substituted porphyrinoids commonly used to form functional assembled systems in Nature yet are still scarcely studied in material chemistry probably due to laborious synthesis of these compounds. In this work β-octa[(4-diethoxyphosphoryl)phenyl]porphyrin (**2HOPPP**) and their metal (Zn(II), Cd(II), Cu(II) and Ni(II)) complexes were prepared in good yields. These highly soluble polyfunctionalized chromophores were characterized in

solution using spectroscopic (NMR, UV–vis, fluorescence), electrochemical and spectroelectrochemical methods. Attachment of the highly electron-withdrawing group (EWG) $P(O)(OEt)_2$ to the porphyrin macrocycle leads to easier reductions and harder oxidations of the macrocycle for all complexes as compared to corresponding *meso*-tetra(diethoxyphosphorylphenyl)porphyrin derivatives reported previously. We demonstrated that the strong electron deficient character of the **MOPPP** porphyrins results principally from the increase in the number of EWG at the periphery of the tetrapyrrolic macrocycle. Electron deficient porphyrins are highly required in supramolecular and material chemistry in part due to their ability to form supramolecular assemblies *via* the coordination of axial ligands to the central metal atom. According single crystal X-ray data, **ZnOPPP** forms in the crystalline phase unusual mutually coordinated dimers in which two tetrapyrrolic macrocycles are connected through hydrogen bonding of two phosphoryl groups and water molecules axially coordinated to the zinc atoms of the partner molecule. The involvement of water molecules in porphyrin binding allows for an increase of distance between two porphyrin mean N_4 planes, up to 4.478 Å. The off-set of phosphoryl groups attached to the macrocycle through a 1,4-phenylene spacer withdraws the whole porphyrin macrocycle of one molecule from spatial overlap with the macrocycle of a partner molecule and increases the Zn–Zn distance up to 10.372 Å. This still unknown type of porphyrin dimers allows to get deeper insight in the organization of naturally occurring tetrapyrrolic macrocycles.

1. INTRODUCTION

Porphyrins are widely studied and increasingly attracting interest in material science, physics, biology and medicine. The interest in these compounds comes from their amazing diversity of functions in the naturally occurring tetrapyrrolic macrocycles, these functions being performed after subtle modification of the macrocycle periphery and their environment

in biological systems.[1] It is now well-known that using artificial compounds we can learn more about natural processes and also employ their optical, electron transfer and catalytic properties to delivery societally important research outputs. Accordingly, porphyrin synthesis is an important starting point for many academic and industrial scholars. Unfortunately, the design of functional porphyrins exhibiting target properties is still limited by the synthetic availability of tetrapyrrolic macrocycles. In fact, among artificial porphyrins, only symmetrical *meso*-substituted porphyrins of A_4- and A_2-types are readily available.[2,3] Synthetic approaches to unsymmetrically substituted porphyrins, similar to those found in nature, are more sophisticated and have attracted more and more attention over the past decades.[4-9] Recently, a new dimension appeared in porphyrin chemistry and many research groups focused their studies on multi-porphyrin assemblies because nanoscale porphyrin dimers and oligomers may leads to specific functions as is observed in natural photosynthesis. It was demonstrated that porphyrin assemblies provide potential electron- and/or energy-transfer molecular materials,[10-15] photoinduced molecular switches,[16] optical sensors,[17-21] catalysts [22,23] and targets with biological interest.[24,25] These multi-porphyrin systems can be prepared by covalent binding of several tetrapyrrolic macrocycles or through the organization of supramolecular assemblies using weak intermolecular interactions.[26,27] Conventional synthetic strategies to prepare covalently bonded multi-chromophores are generally tendinous and always result in a low product yield.[28,29] A key role of supramolecular chemistry in the development of multi-porphyrin systems results from unique structural features of the porphyrin molecule. Their large aromatic system fits well with stabilization of supramolecular systems through π-π stacking and offers numerous synthetic pathways to introduce functional groups at their periphery which can reinforce the molecular assembly addressing weak interactions of different types such as hydrogen bonding or van der Waals contacts, for instance. Moreover, metal complexes with porphyrin ligands allow for metal-mediated

assembly through coordinative bonding. Being weak in nature, the non-covalent interactions must be numerous to give stable 1D, 2D or 3D species with nano-sized dimensions such as tubes, rods, sheets and so on.[30,31] Polyfunctionalized porphyrins structurally optimized to the requirements of supramolecular chemistry are still scarce, in part because porphyrin synthesis was focused for a long time on the selective introduction of single specific substituent at the target position of the porphyrin macrocycle. The preparation of porphyrins compatible with principles of multi-point molecular recognition are attracting a growing interest in recent research works.[30,31]

To increase the number of functional groups at the macrocycle periphery, β-positions of the macrocycle are promising since eight functional groups can be introduced to obtain highly symmetric molecules. However, many β-octa-substituted porphyrins have a non-planar macrocyclic core and exist in various conformation that complicates the molecular recognition processes. The first attempts to prepare 2,3,7,8,12,13,17,18-octaarylporphyrins have shown that these compounds are flat but exhibit a very low solubility in all organic solvents that strongly limits their usefulness. We assumed that this drawback can be overcome by introduction of hydrophilic diethylphosphoryl ($P(O)(OEt)_2$) groups on the aryl substituents of these compounds. Dialkoxyphosphoryl-substituted metalloporphyrins are of interest as molecular building blocks in supramolecular chemistry because these complexes with electron deficient macrocycles exhibit a high affinity to axial ligation and the $P(O)(OEt)_2$ group possesses three Lewis basic sites which can participates in the formation of supramolecular networks. Moreover, these groups can be easily transformed into corresponding acids or mono-esters which are excellent molecular precursors for synthesis of coordination polymers including MOFs. Up to now, among the known polyphosphonate porphyrin derivatives, only the bis- and tetra-substituted macrocycles have been widely studied and, in most of them, the $P(O)(OR)_2$ groups (R = H, Alk) are located at the *meso*-

positions of the tetrapyrrolic macrocycle being directly bonded to the macrocycle or separated by 1,4-phenylene or acetylene linkers.[32-35] The supramolecular assembly of a nucleoside and an octa-phosphonate derivative of *meso*-tetraphenylporphyrin bearing two phosphonate groups in each phenyl substituent was recently investigated.[36] Our initial attempts to prepare porphyrins with four $P(O)(OEt)_2$ substituents at the β-positions of the macrocycle failed, revealing that this functionalization is more delicate as compared to the preparation of *meso*-substituted derivatives and required specific synthetic methods.[37]

In this work we have investigated synthetic approaches to obtain the porphyrins **MTPPP(PO$_3$Et$_2$)$_8$** and **MOPPP** (Figure 1) in which eight diethoxyphosphoryl ($P(O)(OEt)_2$) groups were attached to β-positions of the macrocycle directly or through a 1,4-phenylene linker, respectively.

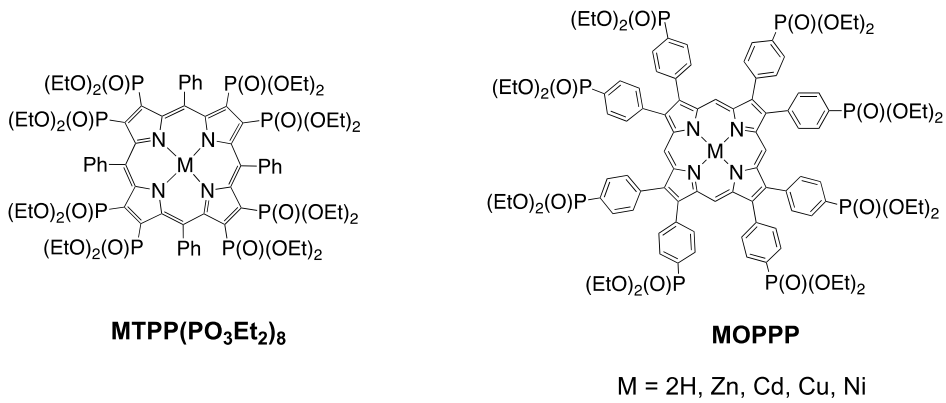

Figure 1. Octa-β-phosphonate-substituted porphyrins investigated in this work.

We developed a gram-scale synthesis of the electron-deficient porphyrin **2HOPPP** and demonstrated that the insertion of various metal ions such as Zn(II), Cd(II), Ni(II) and Cu(II) in this ligand proceeds smoothly, affording the corresponding metallocomplexes **MOPPP** in high yields which were characterized by spectroscopic, electrochemical and spectroelectrochemical techniques. We also shown that zinc complex **ZnOPPP** forms unusual dimers in the crystalline phase in which the two tetrapyrrolic macrocycles are assembled through hydrogen bonding of two $P(O)(OEt)_2$ groups to water molecules which in tune are

axially coordinated to the zinc atoms of the partner molecule. This type of connection of porphyrin molecules is yet unknown despite the assembly of multi-chromophore systems from porphyrin molecules by using molecular recognition methods is attracting a great interest.

2. Results and discussion

2.1. Synthesis of *β*-octa(diethoxyphosphoryl)substituted porphyrin

In the course of this work, we investigated synthetic approaches to *β*-octa(diethoxyphosphoryl)-substituted porphyrins in which phosphorous substituents are attached to the macrocyclic core directly or through a 1,4-phenylene linker as shown in Figure 1 (**TPP(PO$_3$Et$_2$)$_8$** and **OPPP** series, respectively).

Two synthetic methodologies are widely used for the preparation of functionalized porphyrins. The first consists of the cyclization of aldehydes with pyrroles followed by the oxidation of the porphyrinogens thus obtained.[3-5] The second approach is based on the modification of a pre-formed porphyrin backbone. In particular, transition-metal-catalyzed carbon-carbon and carbon-heteroatom (N, O, S, Se, P, B) bond forming reactions are widely used in the frame of this strategy.[6-9] Among them, the transformation of bromoporphyrins into dialkyl phosphonate-substituted derivatives was reported for both *meso*- and *β*-substituted derivatives.[37,38]

In our preliminary experiments, 2,3,7,8,12,13,17,18-octabromo-5,10,15,20-tetraphenylporphyrin **2HTPPBr$_8$** was chosen as a starting compound to prepare the phosphonate containing porphyrin **2HTPP(PO$_3$Et$_2$)$_8$** because this porphyrin is readily available from commercial **TPP** by a standard bromination procedure.[39-41] Unfortunately, when the reaction of **2HTPPBr$_8$** with diethyl H-phosphonate was performed in the presence

of the copper iodide/*N,N'*-dimethyldiaminoethane catalytic system and cesium carbonate as a base at reflux under Ar (Scheme 1), the target product was not obtained.

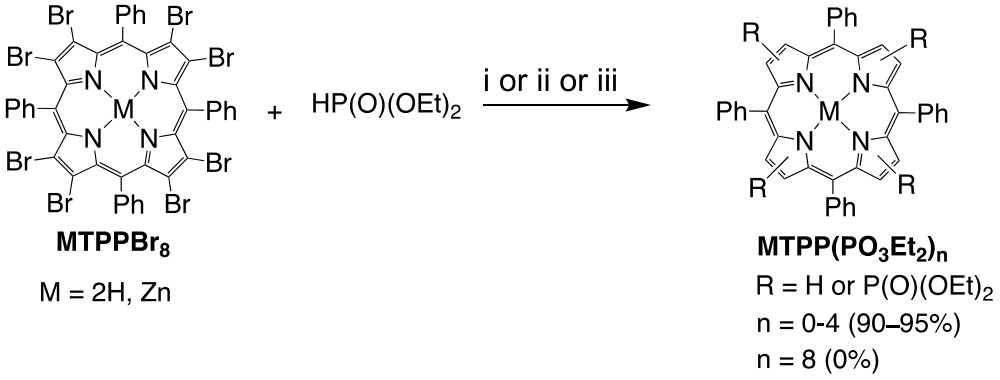

Scheme 1. Transition metal-mediated phosphonylation of porphyrins **MTPPBr$_8$**. General conditions: i) 5–25 equiv of $HP(O)(OEt)_2$, 0.2–3 equiv of CuI, 0.5–25 equiv of $MeNHCH_2CH_2NHMe$, 5–15 equiv Cs_2CO_3, toluene, reflux, Ar; ii) 5–25 equiv of $HP(O)(OEt)_2$, 0.5–1 equiv of $Pd(OAc)_2/3PPh_3$, 15 equiv of NEt_3, toluene, reflux, Ar; iii) 5–25 equiv of $HP(O)(OEt)_2$, 0.5–1 equiv of $[Pd(PPh_3)_4]$, 15 equiv of NEt_3, toluene, reflux.

Despite many attempts to improve the product yield by varying the solvent, the amount of diethyl H-phosphonate, the Cu-based catalytic system and the base, the target product was not prepared even in low yields according to MALDI-TOF MS and NMR analyses of the reaction mixtures. Similar disappointing results were obtained when the Cu catalyst was replaced by the Pd-based catalytic systems ($Pd(OAc)_2/3PPh_3$ and $[Pd(PPh_3)_4]$) and triethylamine was added as a base. The phosphonylation of **2HTPPBr$_8$** was observed in this case but afforded a complex mixture of the compounds **2HTPP(PO$_3$Et$_2$)$_n$** (n = 0–4) according to MALDI-TOF MS analysis. Multi-component mixtures of regio-isomeric porphyrins **2HTPP(PO$_3$Et$_2$)$_n$** containing up to four phosphorous substituents formed under these conditions were inseparable by column chromatography. Noteworthy, products which should be formed in the course of the stepwise phosphonylation of **2HTPPBr$_8$** (e. g. **2HTPPBr$_7$(PO$_3$Et$_2$)**, **2HTPPBr$_6$(PO$_3$Et$_2$)$_2$** and so on) were never observed in the reactions

studied. This indicates that the dibromo-substituted pyrrole units of the **2HTPPBr$_8$** macrocycle were not subject to phosphonylation by diethyl H-phosphonate but were reduced in the course of the hydrodebromination reaction. This side reaction has been commonly observed in the phosphonylation of porphyrins.[37,38] Similar results were reported previously for phosphonylation of the 2,3,12,13-tetrabromo-5,10,15,20-tetraphenylporphyrin (**2HTPPBr$_4$**) with diethyl H-phosphonate in the presence of Pd catalysts.[37] This distinguishes the studied C–P bond forming reaction from many transition metal-catalyzed transformations of *β*-poly(bromo)-substituted porphyrins such as the Stille and the Suzuki reactions, for instance, which were successfully used for one-pot octa-functionalization of the macrocycle.[42,43]

When the free base porphyrin **2HTPPBr$_8$** was replaced by its Zn complex, the reactions with diethyl H-phosphonate gave similar disappointed results in all conditions discussed above as shown in Scheme 1.

Thus, we changed the synthetic methodology and decided to introduce the phosphorus substituents in the pyrrole ring before formation of the porphyrin ring. *N*-(phenylsulfonyl)-2,3-dibromopyrrole (**1**) was prepared according to previously reported procedure[44] in 27% yield and introduced in the Cu- or Pd-mediated cross-coupling reaction with diethyl H-phosphonate as shown in Scheme 2. Surprisingly, bisphosphonate **3** was not obtained and the hydrodebromination reaction was predominant under all studied experimental conditions. The heterocoupling reaction gave the maximum product yield, being performed with 10 mol% of $Pd(OAc)_2/3PPh_3$ in refluxing ethanol. However, even under these conditions only mono-phosphonylated product **2** was obtained in low (27%) yield.

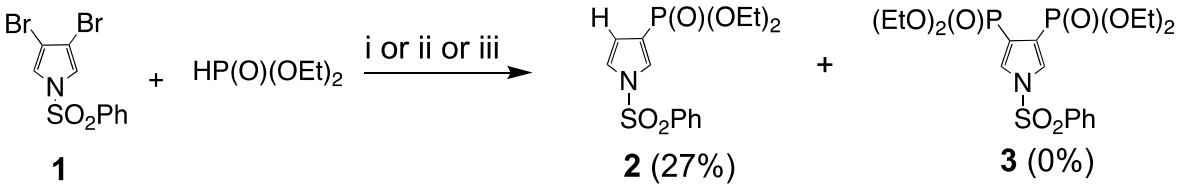

1 **2** (27%) **3** (0%)

Scheme 2. Transition metal-mediated phosphonylation of dibromopyrrole **1**. General conditions: i) 2.2–5.0 equiv of $HP(O)(OEt)_2$, 0.2–1 equiv of CuI, 0.5–5 equiv of $MeNHCH_2CH_2NHMe$, 2.5–5.0 equiv of Cs_2CO_3, toluene, reflux, Ar; ii) 2.2–5.0 equiv of $HP(O)(OEt)_2$, 0.1–0.5 equiv of $Pd(OAc)_2/3PPh_3$, 2.5 equiv of NEt_3, toluene or ethanol, reflux, Ar; iii) 2.2–5.0 equiv of $HP(O)(OEt)_2$, 0.5–1 equiv $[Pd(PPh_3)_4]$, 2.5 equiv of NEt_3, toluene or ethanol, reflux.

Next, we studied the synthesis of **2HOPPP** in which phosphonate substituents and the macrocycle are separated by a 1,4-phenylene linkers (Figure 1). We focused on the step-wise synthesis of **2HOPPP** from the $P(O)(OEt)_2$-substituted pyrrole (Schemes 3–5) because a very low solubility of the *β*-octabromo-substituted porphyrins **2HTPPBr$_8$** and **ZnTPPBr$_8$** is inconvenient for their use in gram-scale synthesis of porphyrins. Accordingly, 3,4-bis(4-bromophenyl)-*1H*-pyrrole-2,5-dicarboxylic acid **4** was prepared by the condensation of 4,4′-dibromobenzil (**5**) and dimethyl *N*-acetyliminodiacetate (**6**) followed by deprotection of the pyrrole ring and hydrolysis of ester groups performed without purification of the intermediate compounds (Scheme 3). The condensation reaction was carried out by refluxing compounds **5** and **6** for 30 min in the presence of sodium methylate in methanol. It was shown that the yield of pyrrole **4** was highly dependent on the reagent ratio and increased from 27% to 53% when iminodiacetate **6** was taken in two-fold excess. However, further increase of the amount of this compound up to 3 equiv. had a detrimental effect and the target product was obtained in 10% yield. The reaction time is another parameter which allows for the reaction optimization. After prolonging the reflux from 30 min to 40 min, the pyrrole **4** was obtained in 64% yield. Decarboxylation of compound **4** smoothly proceeds in refluxing ethanolamine yielding pyrrole **7** in 81% yield.

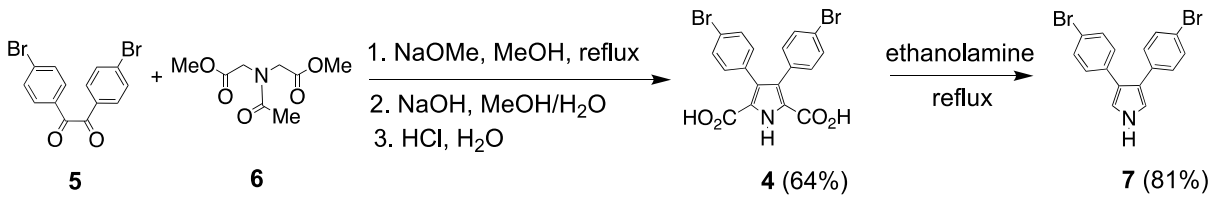

Scheme 3. Synthesis of 3,4-bis(4-bromophenyl)-*1H*-pyrrole (**7**).

The Hirao reaction with dibromide **7** was firstly performed with the protected pyrrole **8** (Scheme 4). The reaction proceeded smoothly and gave the product in 57% yield only when compound **8** and diethyl H-phosphonate were reacted in the presence of 30 mol% $Pd(OAc)_2/3PPh_3$ and triethylamine in refluxing ethanol. In contrast, when this transformation was performed in toluene, the product yield was as low as 9%. Unfortunately, both the protection of pyrrole **7** and the deprotection of the $P(O)(OEt)_2$-substituted pyrrole **9** were shown to be delicate. For instance, our attempt to deprotect pyrrole **9** by refluxing a THF solution of this compound in the presence of tetrabutylammonium fluoride (TBAF) gave the product **10** in only 45% yield.

Much to our satisfaction, we later found that the non-protected pyrrole **7** smoothly reacted with diethyl H-phosphonate under these optimized coupling conditions, affording the product **10** in 78–84% yield and this reaction can be successfully scaled up to tens of grams of starting regents (Scheme 4).

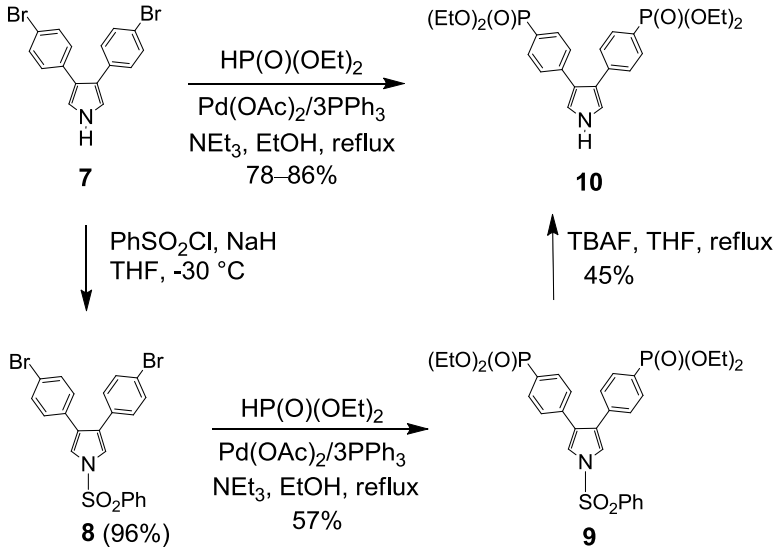

Scheme 4. Synthesis of 3,4-bis[4-(diethoxyphosphoryl)phenyl]-*1H*-pyrrole (**10**).

The synthesis of porphyrin **2HOPPP** was performed by cyclization of pyrrole **10** with formaldehyde in the presence of hydrobromic acid in ethanol followed by the oxidation of the porphyrinogen thus obtained by DDQ in refluxing toluene (Scheme 5) as reported for *β*-octaphenylporphyrin (**2HOPP**).[45] After the introduction of two electron-withdrawing $P(O)(OEt)_2$ substituents at the phenyl rings of the starting pyrrole, the porphyrin yield decreased from 70–80% to 54%, probably due to a more difficult oxidation of the intermediate porphyrinogen or a partial hydrolysis of phosphonate diester groups under acidic conditions. Conducting the oxidation reaction at room temperature, the side hydrolysis was suppressed and the **2HOPPP** product was obtained in 73% yield. Noteworthy, the free base porphyrin **2HOPPP** exhibits a higher solubility than the *β*-octaphenyl-substituted porphyrin **2HOPP** in chlorinated solvents ($CHCl_3$, CH_2Cl_2) and many other organic solvents, thus simplifying its purification by column chromatography.

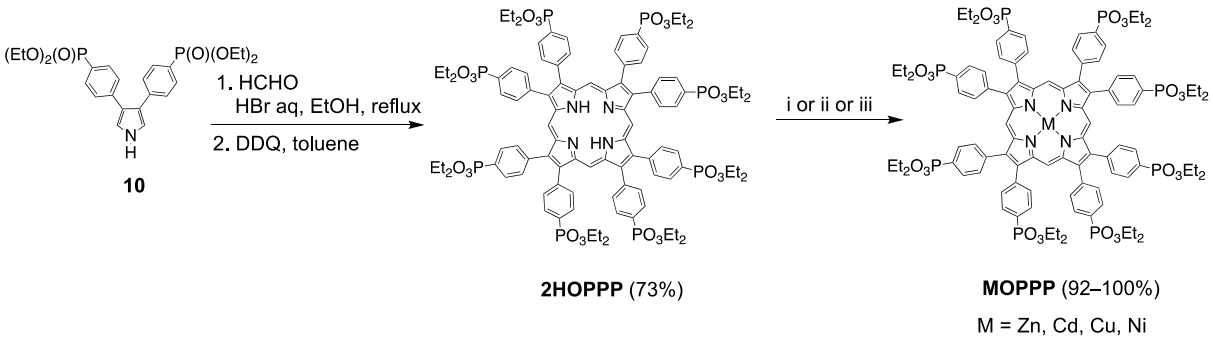

Scheme 5. Synthesis of octa(phosphonate diester)-substituted porphyrin **2HOPPP** and its metal complexes **MOPPP**. Reagents and conditions: i) $M(OAc)_2$ (M = Zn(II), Cu(II)); $CHCl_3$/MeOH; reflux; ii) $Ni(acac)_2$ (acac = acetylacetonate), toluene, reflux; iii) $Cd(NO_3)_2$, NaOAc, $CHCl_3$/MeOH.

Due to the electron-deficient character of this porphyrin ligand and its good solubility in common organic solvents, the insertion of diverse metal ions in this macrocycle smoothly

proceeds under standard conditions reported elsewhere in the literature for the *meso*-tetra(phenyl)porphyrin (**TPP)**. In the course of our studies, we successfully prepared complexes with redox inactive Zn(II), Ni(II), Cu(II) and Cd(II) ions (Scheme 5). Zn(II) and Cu(II) complexes were obtained using metal acetate salts as a metal source in a $CHCl_3/CH_3OH$ solvent mixture. Insertion of Ni(II) ions required nickel acetylacetonate as a metal source and a high temperature which was achieved using refluxing toluene as a solvent medium. The Cd(II) complex was obtained using a nitrate salt after addition of sodium acetate for buffering the reaction mixture. The all complexes were prepared in high yields (> 90%) after purification by column chromatography.

The UV–vis and ^{1}H NMR spectroscopic studies of these complexes were performed to prove their purity and get insight into their structural parameters and self-assembly in solution (Figures S2,S3, S7–S33, see Supporting Information). It is well-known that dodecaphenyl-substituted metalloporphyrins (**DcPP**) bearing substituents in all *meso*- and β-positions of the tetrapyrrolic macrocycle exhibit non-planar deformations of the tetrapyrrolic macrocycle observable as characteristic bathochromic shifts of absorption bands in UV–vis spectra.[46,47] The UV–vis spectra of the β-octaaryl-substituted derivatives (**OPP**) led us to conclude that the tetrapyrrolic macrocycle was flat in these compounds as in the case of the free base **TPP** porphyrin and their complexes.[45,48] Electronic absorption spectra of the newly synthesized free base porphyrin **2HOPPP** and its complexes in $CHCl_3$/MeOH solution are presented in Figure S12, S18, S24, S30 and S33 and summarized in Table 1. The data reported for free base porphyrins **2HDcPP** and **2HOPP** and their complexes are also included in Table 1 for comparison reasons.

As shown in Figure S12 and Table 1, **2HOPPP** exhibits light absorption typical for porphyrins with an intense Soret band (428 nm) and four Q bands in the region of 517–639 nm. The number of Q bonds is expectedly decreased from four to two after insertion of

Cu(II), Ni(II) and Zn(II) ions in the tetrapyrrolic macrocycle. The spectrum of **CdOPPP** in the Q-region is more complicated and two intense bands are accompanied by two absorption bands of low intensities. The Soret bands of **CuOPPP** and **NiOPPP** appears at 425 and 422 nm, respectively, while a bathochromic shift of this band to 440 and 448 nm are observed in the spectra of **ZnOPPP** and **CdOPPP**, respectively. The Soret bands of ruffled tetrapyrrolic macrocycles belonging to the **DcPP** series were observed at 448–460 nm.[46,47] These data reveal that the porphyrin ring in **NiOPPP** and **CuOPPP** is almost flat as it was already proposed for the **OPP** porphyrins based on their UV–vis spectroscopic data and semi-empirical PM3 calculations.[48,49] In contrast, we cannot exclude that **ZnOPPP** and **CdOPPP** have a ruffled macrocycle as it was observed in **DcPP** series.

The UV–vis spectra of free base porphyrin **2HOPPP** and their complexes in $CHCl_3$/MeOH are not concentration dependent. In contrast, an increase of the concentration of **ZnOPPP** in chloroform leads to a bathochromic shift or broadening of all absorption bands (Figure S2). The Soret band shifts by only 1 nm and broadening when the **ZnOPPP** concentration increased from 2.7 x 10^{-7} to 3.4 x10^{-5} M. The shifts of Q-bands can be investigated over a larger concentration range due to the lower intensity of these bands. When the compound concentration was increased from 2.7 x10^{-7} to 4.3 x 10^{-4} M significant shifts (from λ = 561 up to 551 nm, $\Delta\lambda$ = 10 nm and from λ = 586 up to 597 nm, $\Delta\lambda$ = 11 nm) of Q-bands were observed indicating that molecular association takes place under the studied solution conditions (Figure S1). This association is also seen by NMR spectroscopy because all proton signals are broadened when the spectrum of **ZnOPPP** is recorded in $CDCl_3$ solution (Figure S2). Addition of only 5μL of methanol to the studied $CDCl_3$ solution led to a downfield shift of all proton signals which now appeared as sharp signals and gave an expected coupling pattern. It is worth noting that such solution behavior was reported for Zn(II) porphyrins with $P(O)(OEt)_2$ substituents directly attached to *meso*- or *β*-positions of the

porphyrin ring.[37,38] However, in contrast to these compounds, the structure of **ZnOPPP** aggregates cannot be determined using NMR analysis because of the signal broadening.

Table 1. UV–vis spectroscopic data for porphyrins **MOPPP** and referenced compounds **DPP** and **OPP** series.

Compound	Solvent	λ_{abs} (nm) (log ε)	
2HOPPP	$CHCl_3$/MeOH (2:1, v/v)	428 (5.28), 517 (4.37), 552 (4.10), 585 (3.98), 639 (3.62)	this work
2HOPP	$CHCl_3$	423, 515, 551, 583, 635	45 49
	$CHCl_3$	423 (5.13), 518 (4.23), 550 (4.04), 583 (3.95), 635 (3.47)	
2HDcPP	DMF	479 (5.00), 571 (3.56), 645 (3.87), 754 (3.43)	50
ZnOPPP	$CHCl_3$/MeOH (2:1, v/v)	361 (4.15), 440 (5.22), 558 (4.09), 595 (3.92)	this work
ZnOPP	not given	430 (5.40), 554 (4.40), 588 (4.18)	48
CuOPPP	$CHCl_3$/MeOH (2:1, v/v)	347 (4.14), 425 (5.18), 542 (4.00), 579 (4.14)	this work
CuDcPP	toluene	448 (5.24), 580 (4.18), 623 (2.78)	50
CdOPPP	$CHCl_3$/MeOH (2:1, v/v)	448 (5.52), 4.85 (4.13), 525 (4.13), 570 (4.51), 605 (4.13), 664 nm (3.40)	this work
NiOPPP	$CHCl_3$/MeOH (2:1, v/v)	322 (4.35), 359 (4.25), 422 (5.31), 533 (4.21), 569 (4.48)	this work
NiDcPP	CH_2Cl_2	449, 566, 613	47
	piperidine	448, 566, 608	

2.2. Electrochemical studies of β-octaphosphonate-substituted porphyrin 2HOPPP and its metallocomplexes in solution

To define the effect of the $P(O)(OEt)_2$ substituent on electronic structure of the newly synthesized compounds, the free base porphyrin **2HOPPP** and its complexes with redox-inactive Zn(II), Cd(II), Cu(II) and Ni(II) ions were investigated by cyclic voltammetry (CV) in dichloromethane (CH_2Cl_2) containing tetra-*n*-butylammonium perchlorate (TBAP) as supporting electrolyte. The electrochemical data for these porphyrins and reference compounds in the 5,10,15,20-tetraphenyl- (**TPP**) and 5,10,15,20-[tetra(4-(diethoxyphosphoryl)phenyl]porphyrin (**TPPP)** series are summarized in Table 2.

Table 2. Half-wave potentials (V vs. SCE) of investigated octa(diethoxyphosphoryl)-substituted porphyrins and referenced compounds in CH_2Cl_2 containing 0.1 M TBAP.

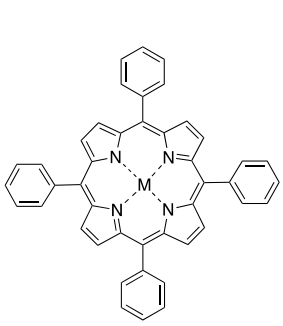

MTPP

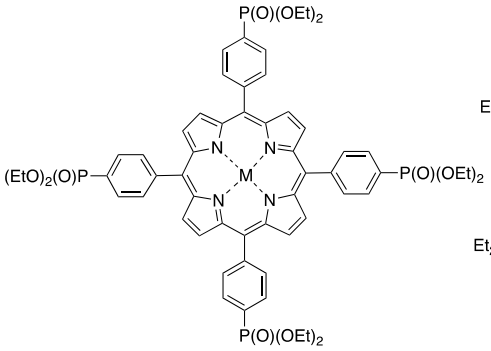

MTPPP

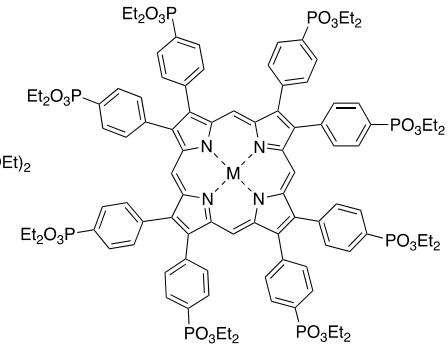

MOPPP

Compound	Oxidation		Reduction		HOMO–LUMO gap (V)	Reference
	2nd ox	1st ox	1st red	2nd red		
2HOPPP	1.71	1.33	–0.95[c]	–1.20	2.28	this work
2HTPPP	1.35	1.18	–1.08	–1.38	2.26	[32]
2HTPP	1.21	1.05	–1.15	–1.50	2.28	[32]
ZnOPPP	1.20	1.05	–1.12	–1.34	2.17	this work
ZnTPPP	1.20	0.90	–1.23	–1.58	2.26	[32]
ZnTPPP[a]	1.29	0.91	–1.28	–1.58	2.26	[51]
ZnTPP	1.07	0.79	–1.34	–1.78	2.13	[32]
CuOPPP	1.40	1.19	–1.04	–1.34	2.23	this work
CuTPPP[a]	1.39	1.14	–1.24	–1.61	2.37	[51]
CuTPP[a]	1.35	0.97	–1.33	–1.71	2.30	[51]
CdOPPP	1.15	1.00	–1.16	–1.50	2.31	this work
NiOPPP		1.18	–1.00	–1.42	2.18	this work
NiTPPP[a]		1.23	–1.20	–1.58	2.51	[51]
NiTPP[a]	1.36	1.02	–1.28	–1.72	2.30	[51]

[a] Electrochemical data (vs Ag/AgCl) in in CH_2Cl_2 containing 0.1 M $TBAPF_6$.

Unfortunately, redox potentials of the Ni(II) and Cu(II) complexes with **TPPP** ligand previously reported in the literature were obtained under different solution conditions that complicate a comparison with our data. Nevertheless, such comparison is still sound because the **ZnTPPP** complex which was investigated under both solution conditions gave very similar results in both solvents.

CV curves for the newly synthesized **MOPPP** compounds are shown in Figure 2. Electrochemistry of the Zn(II), Cu(II) and Cd(II) derivatives can be described in terms of known electrochemical behavior for redox-inactive metal complexes with **TPP** ligands.[52] Two one-electron oxidations and two one-electron reductions corresponding to the formation of π-cation radicals and dication on the oxidation process and π-anion radicals and dianion on reduction are seen in CV curves of these complexes.[52] In contrast, the reversible oxidation of **NiOPPP** proceeds *via* a two-electron transfer process as already reported for other electron-deficient Ni(II) porphyrins.[53,54] Replacement of copper(II) and nickel(II) by more electropositive Zn(II) and Cd(II) ions significantly increases the effective charge density at the macrocycle and the redox potentials are then cathodically shifted as was reported in **TPPP** series.[32,51] For example, the first oxidation and reduction potentials can be turned from 1.02 to 1.18 V and from –1.34 to –1.78 V, respectively, by replacing the Ni(II) central metal ion with the Zn(II).

Comparing redox potentials for complexes with the same metal ions belonging to the **TPP**, **TPPP** and **OPPP** series, it can be seen that attachment of the highly electron-withdrawing group (EWG) $P(O)(OEt)_2$ leads to easier reductions and harder oxidations of the macrocycle for all complexes in the **OPPP** and **TPPP** series as compared to corresponding **TPP** derivatives. As expected, an increase in the number of substituents from four to eight when going from compounds in the **TPPP** to **OPPP** series makes the oxidation more difficult and simplifies the reduction that allows for an increase of available redox potential range. It is interesting to compare the shift of potentials after attachment of one $P(O)(OEt)_2$ substituent at the *meso*- and *β*-positions of the macrocycle. To manage an uncertainty related to experimental conditions, this comparison was done using data for the Zn(II) complexes. The magnitude of shift induced by each substituent in **ZnTPPP** and **ZnOPPP** depends upon the site of electron transfer and varied from 16 to 55 V as shown in Table S2 (see Supporting

Information). We did not observe a systematic cathodic shift of potentials after the change of $P(O)(OEt)_2$ position from *meso*- to *β*- at the macrocycle although the effect of *β*-substituent is higher in most cases. This probably can be rationalized by assuming a different conjugation of the phenyl ring and the macrocycle in the *meso*- and less sterically hindered *β*-substituted derivatives. Thus, the strong electron deficient character of the **MOPPP** porphyrins results principally from the increase in the number of EWG at the periphery of the heterocycle.

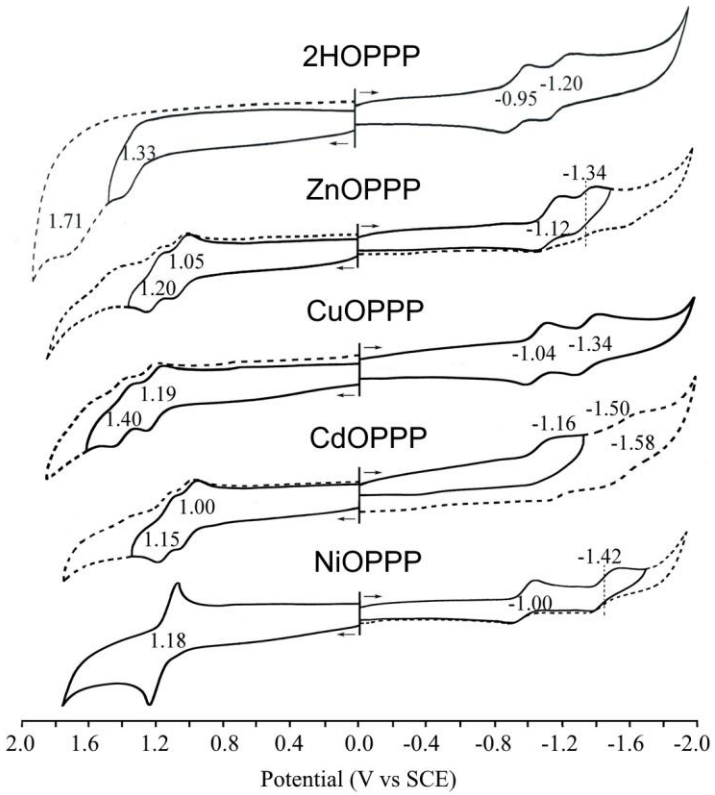

Figure 2. Cyclic voltammograms of porphyrins of **OPPP** series in CH_2Cl_2 containing 0.1 M TBAP.

The oxidation of free base porphyrin **2HOPPP** is more complicated than its metal complexes as shown in Figure 2. Although it has often been proposed that free-base porphyrins undergo two one-electron oxidations to give a π-cation radical and dication, this does not always occur, in particular for electron deficient compounds.[32,55] A disproportionation of singly oxidized species was proposed to occur leading to an increase of the oxidation current.[32] This process has a specific spectroelectrochemical signatures because

it is accompanied by protonation of the macrocycle. To examine the possibility of this process for **2HOPPP**, the electrooxidation of the porphyrin was carried out at controlled potentials and the solution was monitored by thin-layered UV–vis spectroelectrochemistry. The UV–vis spectral changes during the two oxidation processes are shown in Figure 3a and 3b.

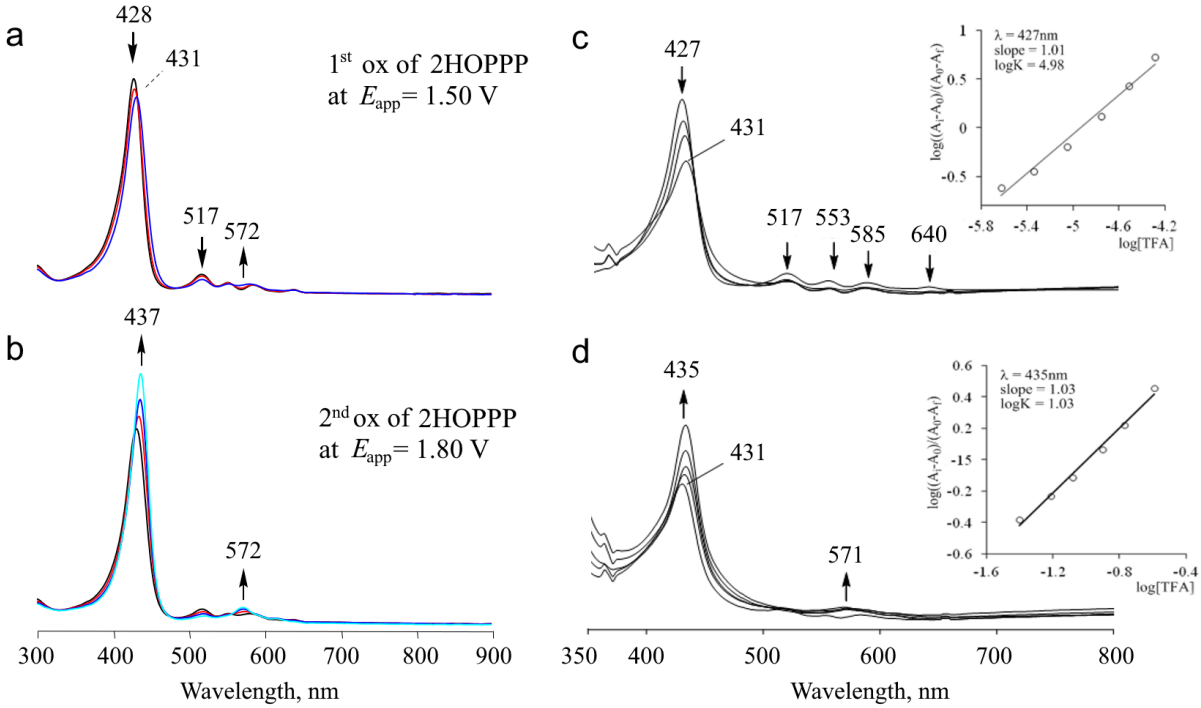

Figure 3. Spectrophotometric changes during controlled potential oxidation of **2HOPPP** in CH_2Cl_2 containing 0.1 M TBAP at (a) E_{app} = 1.50 V and (b) at E_{app} = 1.80 V with comparison to spectral changes during acid titration of **2HOPPP** with TFA (c, d). Insets show the treatment of titration data by using Hill plot method.

UV–vis spectra of the final products reveal the presence of the porphyrin aromatic system after both reactions since the Soret band does not decrease in intensity as would be expected for any products of oxidation of this conjugated π-system. Moreover, the characteristic bathochromic shift and the presence of isosbestic points are typical signatures which were observed during the oxidation of many free base porphyrins, **2HTPPP** being a close analogue to **2HOPPP**.[32] As previously reported for **2HTPPP**, the observed spectral change during oxidation in the thin-layer cell correspond perfectly to the spectral changes

observed during titration of the neutral compound by trifluoroacetic acid TFA. This is also true for **2HOPPP** studied in this work as shown in Figure 3c and 3d. Hill plots for the spectrophotometric titrations are shown in insets of Figures 3c and 3d and have slope of 1.0 with a log K_a = 4.98 and 1.03 for the stepwise addition of two protons. This suggests the formation of protonated porphyrin species after the first and the second oxidations in CH_2Cl_2 in the presence of TBAP. It is worth highlighting that this reaction involving the conversion of the electrooxidized species to a protonated porphyrin with an unoxidized macrocycle is not specific to diethoxyphosphoryl-substituted porphyrins and was observed for instance after the electrooxidation of **2HTPP** and 2,3,7,8,12,13,17,18-octaethylporphyrin (**2HOEP**).[55] Unfortunately, a detailed mechanism of this transformation which formally results in the addition of hydrogen atom to initially formed π-cation radical is still unknown.

The ability of metalloporphyrins in the **OPPP** series to axial coordinate additional ligands was investigated by performing electrochemical studies of **ZnOPPP** in CH_2Cl_2 containing TBAP in the presence and absence of triphenylphosphine oxide ($Ph_3P(O)$) which is known to be an excellent ligand for Zn(II) complexes of **TPPP** and **TPP**.[32] As expected, addition of $Ph_3P(O)$ leads to a change in the electrochemical behavior of the complex inducing formation of a stable ligated complex as shown by cyclic voltammograms in Figure S3 (see Supporting Information).

2.3. Crystal structure of ZnOPPP

2,3,5,7,8,10,12,13,15,17,18,20-dodecaphenylporphyrins (**DcPP**) and their complexes has been intensively studied and single-crystal structures of many derivatives were reported but no 2,3,7,8,12,13,17,18-octaphenylporphyrins (**OPP**) are present in the Cambridge Structural Database and structural parameters of the free base porphyrin **2HOPP** were obtained only by computational calculations using semi-empirical PM3 method.[49]

In the current study, single crystals of porphyrin **ZnOPPP** were obtained by slow evaporation of solvent from a solution of the complex in a $CHCl_3$/MeOH mixture in air at room temperature. The compound crystallizes in the monoclinic space group *C*2/c with one molecule in the asymmetric unit. The zinc atoms adopt a spherical square pyramid geometry with a typical C_{4v} symmetry of ZnN_4O core (Figure 4).

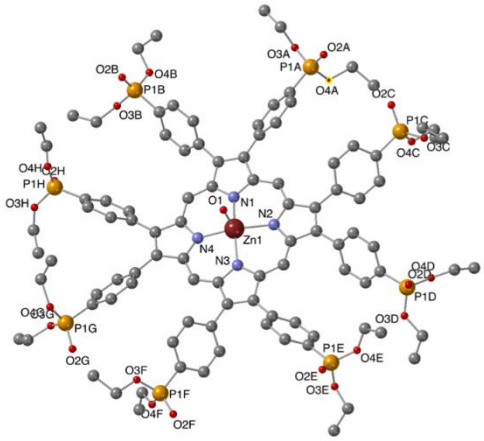

Figure 4. Molecular structure of complex **ZnOPPP**. Hydrogen atoms and minor disordered parts are omitted for clarity.

The four nitrogen atoms of the macrocycle are arranged in the base plane and the apical position is occupied by the oxygen atom of a water molecule which was probably present in trace amounts in the solution used for crystallization. The zinc atom is displaced from the mean porphyrin N_4 plane by 0.293 Å. Such small displacement of the metal atom from the macrocycle towards the axial ligand is a common feature observed in zinc porphyrins bearing one axial ligand.[34,56] The Zn–O distance is significantly shorter (2.087 Å) than that observed in aqua(5,10,15,20-tetraphenylporphyrinato)zinc(II) (2.369 Å), probably due to the electron deficient character of the **2HOPPP** ligand. Thus, both an out-of-plane location of Zn atom and Zn–O distance reveal full-scale coordinative binding the metal center and the water molecule.

The four Zn–N distances (2.076 Å) are in good agreement with corresponding values in Zn(II) complexes of **DcPP** (2.074-2.110 Å).[57] but conformations of the octa- and dodeca-substituted macrocycles are different. In **ZnOPPP**, the heterocycle is almost flat with maximal deviation of the carbon atoms from the mean N_4 plane equal to 0.161 Å. The introduction of four phenyl substituents in *meso*-positions of the porphyrin macrocycle leads to nonplanar distortions of the macrocycle which were the focus of many studies.[58,59] This structural difference is important for supramolecular applications of porphyrins and can be further exploited in the design of flat and highly substituted molecular building blocks with target properties because physico-chemical properties of porphyrins are known to be dependent of the planarity of the macrocycle.[46,47,58,60]

Noteworthy, the twist angle between the phosphonate-substituted aryl substituent and the macrocycle is dependent on the position of aryl group at the macrocycle as can be seen when comparing structures of 5,10,15,20-tetra[(4-(diethoxyphosphoryl)phenyl]porphyrin (**2HTPPP**) and **ZnOPPP**. In **2HTPPP**, all twist angles lie in the range of 62.22–67.79° although only one of the eight corresponding values of the **ZnOPPP** molecule falls in this range; other angles are in the range of 45.46–56.68° which probably points to a decrease of steric hinderance between the phenyl substituents and neighboring atoms in the β-substituted macrocycle.

The most interesting structural feature of the studied compound in the crystalline phase probably is a self-assembly of the porphyrin molecules in mutually coordinated dimers (Figure 5).

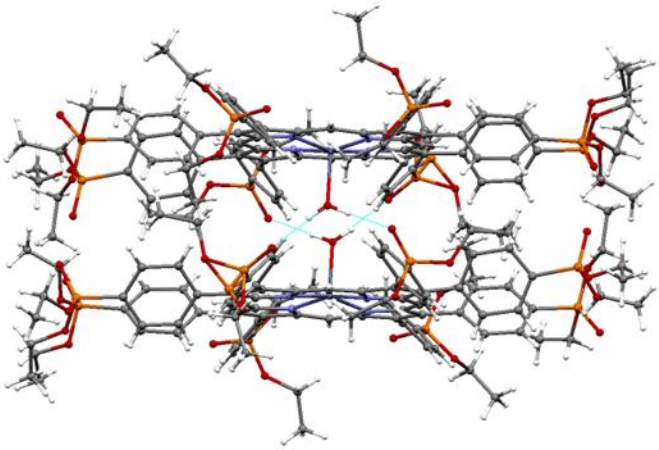

Figure 5. Dimers of the **ZnOPPP** porphyrin formed in crystalline phase. Minor disordered parts are omitted for clarity.

The structure of this dimer is unusual in that the binding of two porphyrin molecules is achieved not through a direct coordination of the phosphoryl oxygen atom to the zinc atom but through the axial coordination to the Zn center of a water molecule which in turn participates in hydrogen bonding of the phosphoryl group belonging to a partner porphyrin molecule. Such hydrogen bonding is possible due to an appropriate distance between adjacent phosphoryl groups attached to neighboring pyrrole rings of the macrocycle. The porphyrin rings are situated in parallel planes as previously observed in mutual dimers of *meso*- and *β*-P(O)$(OEt)_2$-substituted porphyrins in which two porphyrin molecules are linked through two (P)O–Zn bonds.[37,61] The involvement of water molecules in porphyrin binding allows for an increase of distance between two porphyrin mean N_4 planes, up to 4.478 Å, a value significantly higher as compared to the plane separation in all known dimers of P(O)$(OEt)_2$-substituted porphyrins (2.585–3.505 Å). The off-set of phosphoryl groups attached to the macrocycle through a 1,4-phenylene spacer withdraws the whole porphyrin macrocycle of one molecule from spatial overlap with the macrocycle of a partner molecule and increases the Zn–Zn distance up to 10.372 Å.

The dimers of **ZnOPPP** interact in the crystalline phase only through weak intermolecular contacts formed by the hydrogen atoms of phenyl and ethoxy groups (Figure

S4). It is worth noting, that self-assembled porphyrin systems based on octa-substituted tetrapyrrolic macrocycles are limited to a few examples and only one of them has been investigated by single-crystal X-ray analysis to our knowledge.[62-64]

Diethoxyphosphoryl-substituted porphyrins, in which the phosphorous substituent was directly attached to the macrocycle were proposed as models for special pairs in photosynthetic reaction centers.[37,61] From this point of view, dimers obtained in this work can be regarded as models of naturally occurring multi-chromophore architectures involving in electron- and/or energy-transfer of the photosynthesis. To our knowledge, mutual binding of porphyrin molecules in dimers through coordinative and hydrogen bonding was never reported so far.

3. CONCLUSIONS

Development of synthetic approaches to supramolecular porphyrin systems and materials requires specific molecular precursors bearing multiple functional groups at the periphery of the tetrapyrrolic macrocycle to provide multifold binding of porphyrin molecules in nanosized assemblies. We have prepared in gram-scale and in good yield *β*-octa[(4-diethoxyphosphoryl)phenyl]porphyrin, the first porphyrin bearing eight Lewis basic sites at *β*-positions of the macrocycle.

The introduction of the diethyl phosphonate group at the phenyl substituent increases the solubility of *β*-octaphenylporphyrins and significantly changes electronic properties of the tetrapyrrolic macrocycle. We have shown that this ligand easily forms metal complexes with various metal ions and investigated Zn(II), Cu(II), Ni(II) and Cd(II) complexes spectroscopically and electrochemically. These studies reveal the strong electron deficient character of all newly synthesized metalloporphyrins. The presence of eight Lewis base sites at the periphery of the almost planar tetrapyrrolic macrocycle and a high symmetry of these molecules are structural features which are known to be beneficial for supramolecular

assembling. Moreover, electron deficient metalloporphyrins **MOPPP** exhibit a higher affinity to axial ligation as compared to corresponding **TPP** complexes.

We also investigated self-assembly of zinc complex **ZnOPPP** in which the central metal ion can mediate the porphyrin intermolecular binding through the formation of coordinative bonds. In contrast to our expectation to prepare self-assemblies through (P)O–Zn binding which were reported for diverse diethoxyphosphoryl-substituted porphyrins, unusual mutually coordinated dimers were obtained in which two tetrapyrrolic macrocycles are connected through hydrogen bonding of two $P(O)(OEt)_2$ groups to water molecules which are in their turn axially coordinated to the zinc atom of the partner molecule. These self-assembled dimers can be regarded as new model systems of naturally occurring photosynthetic antenna systems.

Based on these first results, we expect that new tetrapyrroles developed in this work being used as diesters, mono-esters or corresponding phosphonic acids will allow for deeper understanding of biological process while also leading to multi-chromophore functional materials for sensing and catalysis. Our ongoing investigation focuses on the synthesis of coordination polymers and thin film materials based on metal complexes with the **2HOPPP** ligand. We expect to prepare stable porous materials and demonstrate how coordinative bonding of the axial ligand can change the structure of porphyrin nano-sized objects deposited on various solid surfaces.

ASSOCIATED CONTENT

The Supporting Information is available free of charge at https://pubs.acs.org/doi/xxx. Experimental Procedures and characterization data provided in the Supporting Information (PDF).

ACKNOWLEDGEMENTS

Ping Chen is acknowledged for assistance with the electrochemical measurements. Marie-José Penouilh, and Marcel Soustelle are warmly acknowledged for their technical support. This work was supported by Russian Science Foundation, Grant № 21-73-00020, We also gratefully acknowledge support from the Robert A. Welch Foundation (K.M.K., Grant E-680), the Centre National de la Recherche Scientifique (CNRS), the Conseil Régional de Bourgogne (PARI IME SMT8 and PARI II CDEA programs), the European Union (European Regional Development Fund, FEDER program).

REFERENCES

(1) *Handbook of Porphyrin Science. Biochemistry of Tetrapyrroles*, Vol. 19, (Eds.: Kadish, K. M.; Smith, K. M.; Guilard R.), World Scientific Press, Singapore, **2012**, p. 399.
(2) *Handbook of Porphyrin Science. Synthetic Developments – Part 1*, Vol. 16, (Eds.: Kadish, K. M.; Smith, K. M.; Guilard R.), World Scientific Press, Singapore, **2012,** p. 403.
(3) Vicente, M. G. H.; Smith, K. M. Syntheses and functionalizations of porphyrin macrocycles. *Curr. Org. Synth.* **2014,** *11*, 3–28.
(4) Vicente, M. G. H. in *The Porphyrin Handbook*, Vol. 1 (Eds.: Kadish, K. M.; Smith, K. M.; Guilard R.), Academic Press, San Diego, **2000**, pp. 149–199.
(5) Senge, M. O. Stirring the porphyrin alphabet soup-functionalization reactions for porphyrins. *Chem. Commun.* **2011,** *47*, 1943–1960.
(6) Setsune, J. Palladium chemistry in recent porphyrin research. *J. Porphyrins Phthalocyanines* **2004,** *8*, 93–102.
(7) Sharman, W. M.; Van Lier, J. E. Use of palladium catalysis in the synthesis of novel porphyrins and phthalocyanines. *J. Porphyrins Phthalocyanines* **2000,** *4*, 441–453.
(8) Shinokubo, H.; Osuka, A. Marriage of porphyrin chemistry with metal-catalysed reactions. *Chem. Commun.* **2009,** 1011–1021.
(9) Hiroto, S.; Miyake, Y.; Shinokubo, H. Synthesis and functionalization of porphyrins through organometallic methodologies. *Chem. Rev.* **2017,** *117*, 2910–3043.
(10) Sugou, K.; Sasaki, K.; Kitajima, K.; Iwaki, T.; Kuroda, Y. Light-harvesting heptadecameric porphyrin assemblies. *J. Am. Chem. Soc.* **2002,** *124*, 1182–1183.
(11) Aratani, N.; Kim, D.; Osuka, A. Discrete cyclic porphyrin arrays as artificial light-harvesting antenna. *Acc. Chem. Res.* **2009,** *42*, 1922–1934.

(12) Harvey, P.; Stern, C.; Gros, C. P.; Guilard, R. The photophysics and photochemistry of cofacial free base and metallated bisporphyrins held together by covalent architectures. *Coord. Chem. Rev.* **2007,** *251*, 401–428.
(13) Uetomo, A.; Kozaki, M.; Suzuki, S.; Yamanaka, K.; Ito, O.; Okada, K. Efficient light-harvesting antenna with a multi-porphyrin cascade. *J. Am. Chem. Soc.* **2011,** *133*, 13276–13279.
(14) de la Torre, G.; Bottari, G.; Sekita, M.; Hausmann, A.; Guldi, D. M.; Torres, T. A voyage into the synthesis and photophysics of homo- and heterobinuclear ensembles of phthalocyanines and porphyrins. *Chem. Soc. Rev.* **2013,** *42*, 8049–8105.
(15) Van Raden, J. M.; Alexandropoulos, D. I.; Slota, M.; Sopp, S.; Matsuno, T.; Thompson, A. L.; Isobe, H.; Anderson, H. L.; Bogani, L. Singly and triply linked magnetic porphyrin lanthanide arrays. *J. Am. Chem. Soc.* **2022**, *144*, 8693–8706.
(16) Yoon, H.; Lim, J. M.; Gee, H.-C.; Lee, C.-H.; Jeong, Y.-H.; Kim, D.; Jang, W.-D. A porphyrin-based molecular tweezer: guest-induced switching of forward and backward photoinduced energy transfer. *J. Am. Chem. Soc.* **2014,** *136*, 1672–1679.
(17) Ogoshi, H.; Mizutani, T.; Hayashi, T.; Kuroda, Y., in *The Porphyrin Handbook*, Vol. 6 (Eds.: Kadish, K. M.; Smith, K. M.; Guilard R.), Academic Press, San Diego, **2000**, pp. 280–340.
(18) Weiss, J. Zinc(II)-porphyrin receptors in multi-point molecular recognition: recent progress. *J. Inclusion Phenom. Macrocyclic Chem.* **2001,** *40*, 1–22.
(19) Hayashi, T.; Aya, T.; Nonoguchi, M.; Mizutani, T.; Hisaeda, Y.; Kitagawa, S.; Ogoshi, H. Chiral recognition and chiral sensing using zinc porphyrin dimers. *Tetrahedron* **2002,** *58*, 2803–2811.
(20) You, L.; Zha, D.; Anslyn, E. V. Recent Advances in supramolecular analytical chemistry using optical sensing. *Chem. Rev.* **2015,** *115*, 7840–7892.
(21) Paolesse, R.; Nardis, S.; Monti, D.; Stefanelli, M.; Di Natale, C. Porphyrinoids for chemical sensor applications. *Chem. Rev.* **2017,** *117*, 2517–2583.
(22) Rizzuto, F. J.; von Krbek, L. K. S.; Nitschke, J. R. Strategies for binding multiple guests in metal-organic cages. *Nat. Rev. Chem.* **2019,** *3*, 204–222.
(23) Gotico, P.; Halime, Z.; Aukauloo, A. Recent advances in metalloporphyrin-based catalyst design towards carbon dioxide reduction: from bio-inspired second coordination sphere modifications to hierarchical architectures. *Dalton Trans.* **2020,** *49*, 2381–2396.
(24) Pan, D.; Liang, P.; Zhong, X.; Wang, D.; Cao, H.; Wang, W.; He, W.; Yang, Z.; Dong, X. Self-assembled porphyrin-based nanoparticles with enhanced near-infrared absorbance for fluorescence imaging and cancer photodynamic therapy. *ACS Appl. Bio Mater*. **2019,** *2*, 999–1005.
(25) Zhang, H.; Bo, S.; Zeng, K.; Wang, J.; Li, Y.; Yang, Z.; Zhou, X.; Chen, S.; Jiang, Z.-X. Fluorinated porphyrin–based theranostics for dual imaging and chemo-photodynamic therapy. *J. Mater. Chem. B* **2020,** *8*, 4469–4474.
(26) Tanaka, T.; Osuka, A. Conjugated porphyrin arrays: synthesis, properties and applications for functional materials. *Chem. Soc. Rev.* **2015,** *44*, 943–969.
(27) *Non-Covalent Multi-Porphyrin Assemblies: Synthesis and Properties*, (Ed: Alessio, E.), Springer Berlin, Heidelberg, **2006**, p. 308.
(28) Burrell, A. K.; Officer, D. L.; Plieger, P. G.; Reid, D. C. W. Synthetic Routes to multiporphyrin arrays. *Chem. Rev.* **2001,** *101*, 2751–2796.
(29) Wang, K.; Osuka, A.; Song, J. Pd-catalyzed cross coupling strategy for functional porphyrin arrays. *ACS Centr. Sci.* **2020,** *6*, 2159–2178.
(30) Beletskaya, I.; Tyurin, V. S.; Tsivadze, A. Y.; Guilard, R.; Stern, C. Supramolecular chemistry of metalloporphyrins. *Chem. Rev.* **2009,** *109*, 1659–1713.

(31) Drain, C. M.; Varotto, A.; Radivojevic, I. Self-organized porphyrinic materials. *Chem. Rev.* **2009,** *109,* 1630–1658.
(32) Kadish, K. M.; Chen, P.; Enakieva, Y. Y.; Nefedov, S. E.; Gorbunova, Y. G.; Tsivadze, A. Y.; Bessmertnykh-Lemeune, A.; Stern, C.; Guilard, R. Electrochemical and spectroscopic studies of poly(diethoxyphosphoryl)porphyrins. *J. Electroanal. Chem.* **2011,** *656,* 61–71.
(33) Uvarova, M. A.; Sinelshchikova, A. A.; Golubnichaya, M. A.; Nefedov, S. E.; Enakieva, Y. Y.; Gorbunova, Y. G.; Tsivadze, A. Y.; Stern, C.; Bessmertnykh-Lemeune, A.; Guilard, R. Supramolecular assembly of organophosphonate diesters using paddle-wheel complexes: first examples in porphyrin series. *Cryst. Growth Des.* **2014,** *14,* 5976–5984.
(34) Lemeune, A.; Mitrofanov, A. Y.; Rousselin, Y.; Stern, C.; Guilard, R.; Enakieva, Y. Y.; Gorbunova, Y. G.; Nefedov, S. E. Supramolecular architectures based on phosphonic acid diesters. *Phosphorus, Sulfur Silicon Relat. Elem.* **2015,** *190,* 831–836.
(35) Rhauderwiek, T.; Wolkersdörfer, K.; Øien-Ødegaard, S.; Lillerud, K.-P.; Wark, M.; Stock, N. Crystalline and permanently porous porphyrin–based metal tetraphosphonates. *Chem. Commun.* **2018,** *54,* 389–392.
(36) Aljabri, M. D.; Jadhav, R. W.; Al Kobaisi, M.; Jones, L. A.; Bhosale, S. V.; Bhosale, S. V. Antenna-like ring structures via self-assembly of octaphosphonate tetraphenyl porphyrin with nucleobases. *ACS Omega* **2019,** *4,* 11408–11413.
(37) Vinogradova, E. V.; Enakieva, Y. Y.; Nefedov, S. E.; Birin, K. P.; Tsivadze, A. Y.; Gorbunova, Y. G.; Bessmertnykh, L. A. G.; Stern, C.; Guilard, R. Synthesis and self-organization of zinc *β*-(dialkoxyphosphoryl)porphyrins in the solid state and in solution. *Chem. Eur. J.* **2012,** *18,* 15092–15104.
(38) Enakieva, Y. Y.; Bessmertnykh, A. G.; Gorbunova, Y. G.; Stern, C.; Rousselin, Y.; Tsivadze, A. Y.; Guilard, R. Synthesis of *meso*-polyphosphorylporphyrins and example of self-assembling. *Org. Lett.* **2009,** *11,* 3842–3845.
(39) Traylor, T. G.; Tsuchiya, S. Perhalogenated tetraphenylhemins: stable catalysts of high turnover catalytic hydroxylations. *Inorg. Chem.* **1987,** *26,* 1338–1339.
(40) Hoffmann, P.; Labat, G.; Robert, A.; Meunier, B. Highly Selective bromination of tetramesitylporphyrin: An easy access to robust metalloporphyrins, M-Br_8TMP and M-Br_8TMPS. Examples of application in catalytic oxygenation and oxidation reactions. *Tetrahedron Lett.* **1990,** *31,* 1991–1994.
(41) Bhyrappa, P.; Krishnan, V. Octabromotetraphenylporphyrin and its metal derivatives: Electronic structure and electrochemical properties. *Inorg. Chem.* **1991,** *30,* 239–245.
(42) Chandra, T.; Kraft, B. J.; Huffman, J. C.; Zaleski, J. M. Synthesis and structural characterization of porphyrinic enediynes: geometric and electronic effects on thermal and photochemical reactivity. *Inorg. Chem.* **2003,** *42,* 5158–5172.
(43) Bhyrappa, P.; Sankar, M.; Varghese, B. Mixed substituted porphyrins: Structural and electrochemical redox properties. *Inorg. Chem.* **2006,** *45,* 4136–4149.
(44) Fukuda, T.; Sudo, E.; Shimokawa, K.; Iwao, M. Palladium-catalyzed cross-coupling of N-benzenesulfonyl-3,4-dibromopyrrole and its application to the total syntheses of lamellarins O, P, Q, and R. *Tetrahedron* **2008,** *64,* 328–338.
(45) Takeda, J.; Ohya, T.; Sato, M. A new synthesis of octaarylporphyrin: naturally occurring porphyrin mimics. *Chem. Pharm. Bull.* **1990,** *38,* 264–266.
(46) Alden, R. G.; Crawford, B. A.; Doolen, R.; Ondrias, M. R.; Shelnutt, J. A. Ruffling of nickel(II) octaethylporphyrin in solution. *J. Am. Chem. Soc.* **1989,** *111,* 2070–2072.
(47) Shelnutt, J. A.; Medforth, C. J.; Berber, M. D.; Barkigia, K. M.; Smith, K. M. Relationships between structural parameters and Raman frequencies for some planar and nonplanar nickel(II) porphyrins. *J. Am. Chem. Soc.* **1991,** *113,* 4077–4087.

(48) Ono, N.; Miyagawa, H.; Ueta, T.; Ogawa, T.; Tani, H. Synthesis of 3,4-diarylpyrroles and conversion into dodecaarylporphyrins; a new approach to porphyrins with altered redox potentials. *J. Chem. Soc., Perkin Trans. 1* **1998,** 1595–1602.
(49) Pukhovskaya, S. G.; Efimovich, V. A.; Semeikin, A. S.; Golubchikov, O. A. Kinetics of the formation of copper β-octaphenylporphyrin complexes in pyridine and acetic acid. *Russ. J. Inorg. Chem.* **2010,** *55*, 1494–1498.
(50) Takeda, J.; Ohya, T.; Sato, M. A ferrochelatase transition-state model. Rapid incorporation of copper(II) into nonplanar dodecaphenylporphyrin. *Inorg. Chem.* **1992,** *31*, 2877–2880.
(51) Kumar, R.; Yadav, P.; Kumar, A.; Sankar, M. Facile synthesis and electrochemical studies of diethoxyphosphorylphenyl-substituted porphyrin and its metal complexes. *Chem. Lett.* **2015,** *44*, 914–916.
(52) K. M. Kadish, G. Royal, E. Van Caemelbecke, L. Gueletti, in *The Porphyrin Handbook*, Vol. 9 (Eds.: K. M. Kadish, K. M. Smith, R. Guilard), Academic Press, San Diego, CA, **2000**, pp. 1–219.
(53) Ghosh, A.; Halvorsen, I.; Nilsen, H. J.; Steene, E.; Wondimagegn, T.; Lie, R.; van Caemelbecke, E.; Guo, N.; Ou, Z.; Kadish, K. M. Electrochemistry of nickel and copper *β*-octahalogeno-*meso*-tetraarylporphyrins. Evidence for important role played by saddling-induced metal($d_{x^2-y^2}$)−Porphyrin("a_{2u}") orbital interactions. *J. Phys. Chem. B* **2001,** *105*, 8120–8124.
(54) Kumar, R.; Sankar, M. Synthesis, spectral, and electrochemical studies of electronically tunable *β*–substituted porphyrins with mixed substituent pattern. *Inorg. Chem.* **2014,** *53*, 12706–12719.
(55) Inisan, C.; Saillard, J.-Y.; Guilard, R.; Tabard, A.; Le Mest, Y. Electrooxidation of porphyrin free bases: fate of the π-cation radical. *New J. Chem.* **1998,** *22*, 823–830.
(56) Bessmertnykh-Lemeune, A. G.; Guilard, R.; Stern, C.; Enakieva, Y.; Gorbunova, Y.; Tsivadze, A.; Nefedov, S. E., Biomimetic studies of porphyrin self-assembled systems. in *Supramolecular Systems: Chemistry, Types and Applications* (Ed.: C. Pena), Nova Science Publishers, New York, **2017**, pp. 93–181.
(57) Kojima, T.; Nakanishi, T.; Honda, T.; Harada, R.; Shiro, M.; Fukuzumi, S. Impact of distortion of porphyrins on axial coordination in (porphyrinato)zinc(II) complexes with aminopyridines as axial ligands. *Eur. J. Inorg. Chem.* **2009,** *2009*, 727–734.
(58) Medforth, C. J.; Senge, M. O.; Smith, K. M.; Sparks, L. D.; Shelnutt, J. A. Nonplanar distortion modes for highly substituted porphyrins. *J. Am. Chem. Soc.* **1992,** *114*, 9859–9869.
(59) Harada, R.; Matsuda, Y.; Ōkawa, H.; Miyamoto, R.; Yamauchi, S.; Kojima, T. Synthesis and characterization of chromium(III) octaphenylporphyrin complexes with various axial ligands: An insight into porphyrin distortion. *Inorg. Chim. Acta* **2005,** *358*, 2489–2500.
(60) Senge, M. O.; MacGowan, S. A.; O'Brien, J. M. Conformational control of cofactors in nature – the influence of protein–induced macrocycle distortion on the biological function of tetrapyrroles. *Chem. Commun.* **2015,** *51*, 17031–17063.
(61) Matano, Y.; Matsumoto, K.; Terasaka, Y.; Hotta, H.; Araki, Y.; Ito, O.; Shiro, M.; Sasamori, T.; Tokitoh, N.; Imahori, H. Synthesis, structures, and properties of *meso*–phosphorylporphyrins: Self–organization through P–Oxo–Zinc coordination. *Chem. Eur. J.* **2007,** *13*, 891–901.
(62) Masuoka, N.; Itano, H. A. Radical intermediates in the oxidation of octaethylheme to octaethylverdoheme. *Biochemistry* **1987,** *26*, 3672–3680.
(63) Balch, A. L.; Noll, B. C.; Reid, S. M.; Zovinka, E. P. Coordination patterns for oxophlorin ligands. Pyridine-induced cleavage of dimeric manganese(III) and iron(III) octaethyloxophlorin complexes. *Inorg. Chem.* **1993,** *32*, 2610–2611.

(64) Senge, M. O.; Smith, K. M. Axial coordination phenomena in highly substituted porphyrins. Crystal structure of the polymeric (2,3,7,8,12,13,17,18-octaethyl-5,10,15,20-tetranitroporphyrinato)zinc(II), [{Zn(oetnp)}$_n$]. *J. Chem. Soc., Chem. Commun.* **1994,** 923–924.

Table of content

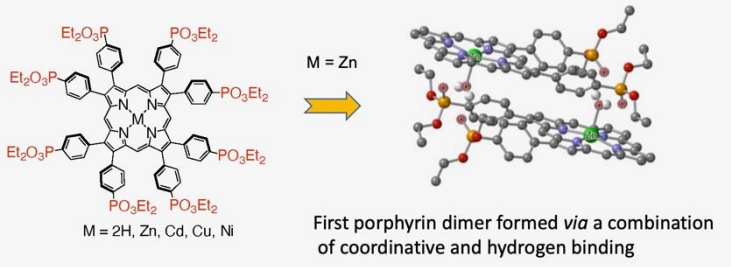

Synopsis

β-Octa[(4-diethoxyphosphoryl)phenyl]porphyrin (**2HOPPP**) and their metal (Zn(II), Cd(II), Cu(II) and Ni(II)) complexes were prepared in good yields. Strong electron deficient character of the **2HOPPP** porphyrin was demonstrated by electrochemical measurements. **ZnOPPP** forms in the crystalline phase unusual mutually coordinated dimers in which two tetrapyrrolic macrocycles are connected through hydrogen bonding of two phosphoryl groups and water molecules axially coordinated to the zinc atoms of the partner molecule.